Infrared Physics & Technology 71 (2015) 501–505

Contents lists available at ScienceDirect

Infrared Physics & Technology

journal homepage: www.elsevier.com/locate/infrared

Brief Report

Analysis on the selection of optimal ADC parameters in indirect measurement

Xiaoming Zhu [a,b], Xiaodong Wang [a,*], Zhijun Xu [a], Bingyu Li [a]

[a] Changchun Institute of Optics, Fine Mechanics and Physics, Chinese Academy of Sciences, Changchun 130033, China
[b] University of Chinese Academy of Sciences, Beijing 100049, China

HIGHLIGHTS

- Providing a reference of ADC parameters selection in indirect measurement.
- Showing several significant ADC parameters' effects on indirect measurement.
- Setting a guideline of ADC selection for CRDS.

ARTICLE INFO

Article history:
Received 17 April 2015
Available online 6 May 2015

Keywords:
CRDS
Signal progressing
ADC

ABSTRACT

How to select optimal ADC parameters in indirect measurement including resolution, sampling rate and sampling error of ADC, and system error is proposed. Fitting of the photo time constant in cavity ring-down spectrum is taken as an example. The effects of resolution, sampling rate and sampling error (with/without system error) of ADC on fitting accuracy are simulated sequentially. The influence of mirror reflectivity on the parameters of fitting functions is analyzed and simulated. Parameters of ADC to distinguish concentration of methane of 1 ppbv at different mirror reflectivity are given.

1. Introduction

Cavity ring-down spectrum (CRDS) is an ultrahigh sensitive and ultraprecise measurement based on characteristic absorption spectrum [1,2]. Three aspects need to be noticed in the case of ultralow concentrations and weak characteristic absorption. Firstly, it should work at clean background band to reduce the impact of other gases, such as methane (1653 nm), carbon dioxide (1603 nm), water vapor (1651 nm) and ammonia gas (1550 nm) [3–7]. Secondly, specular reflection loss should be decreased. Fundamental physical and chemical applications have motivated the improvement of mirror reflectivity from 0.997 to 0.99998, or even higher, accompanying the advancement of detection accuracy from hundreds ppmv to several ppbv, even to pptv middleweight [8–12]. Thirdly, data processing error should be depressed. Data processor develops from analog oscilloscope to analog to digital acquisition card and then to application specific integrated circuit (ASIC) [10,12–14].

Analog digital convertor (ADC) is a bridge connecting analog circuit and digital circuit, and its capability directly determines the performance of apparatus. In most cases, how to select a fine ADC is relatively easy in direct measure design, where only the input level range, resolution, sampling rate, sampling error and sometimes the power dissipation need to be considered [15,16]. It is not straightforward, however, in indirect measurement, such as the exponential time constant measurement. When precise fitting results are expected, it is hard to set a low limit for every parameter of ADC. We could select an excellent one with higher resolution or sampling rate to mitigate (or solve) this problem, but we do not know how excellent it is. Unfortunately, it leads to the improving of minimum operating frequency and the broadening of interface bit-width. And sometimes it may even increase the requirement of the system noise level [17]. Even if all the above are acceptable, however, there still is a doubt whether these performance indexes can satisfy the requirements.

Typically, the digital processing units such as MCU, DSP or ARM, have a very high clock frequency and limited bit-width [18]. Therefore, how to select an optimal ADC whose parameters match well with back-end processing unit is meaningful. The focus of this work is to clarify the relationship between parameter of ADC and

* Corresponding author. Tel.: +86 0431 86708199.
E-mail address: wangxd@ciomp.ac.cn (X. Wang).

http://dx.doi.org/10.1016/j.infrared.2015.04.013
1350-4495/

fitting result. And fitting of the photo time constant in continue wave CRDS is taken as an example.

2. Theory

The experimental setup is shown in Fig. 1(a). A narrow line-width continual wave distributed feedback (CW-DFB) laser works at the characteristic absorption spectrum of the tested gas (here is methane). Laser beam is coupled into the resonant cavity, passing collimator, isolator and mode matching lens sequentially. The cavity length is firstly modulated by piezoelectric ceramics (PZT) to reach resonance. Then the photon intensity inside the cavity rises rapidly to the upper limit of threshold setting, before the laser source is turned off. Photon lifetime is mainly determined by reflection loss of the three super mirrors and the round-trip absorption. The decay curves without/with the sample gas are shown in Fig. 1(b), which can be fitted to obtain the corresponding photo time constant τ_0/τ. According to beer's law and characteristic absorption formula, methane concentration of cavity n_x can be acquired by [2,10,19]:

$$n_x = \frac{1}{c}\left(\frac{1}{\tau} - \frac{1}{\tau_0}\right)/PS(T)\phi(v). \tag{1}$$

where c is the speed of light in vacuum, P is cavity pressure, $S(T)$ is absorption intensity and $\phi(\upsilon)$ is line-shape function.

Imagine an optical resonator whose length is 0.5 m, P is 1 atm, $\phi(\upsilon)$ is 5.13 and $S(T)$ is 0.021 cm^{-2} atm^{-1}. The photo time constant τ is mainly determined by the reflectivity of mirrors and the sample concentration. Table 1 shows the photo time constants τ at different sample concentrations for three kinds of reflectivity of mirrors.

When the reflectivity is 0.99999, fitting accuracy of τ needs to be 15.14 ns to distinguish concentration of methane of 1 ppbv and the corresponding photo time constant is about 56 μs. So far, there is not an explicit parameter to guide our selection of ADC. We compare some mainstream ADC products in order to get the optimal one [20]. Resolution, sampling rate, sampling error and input range of ADC are key parameters, which usually differ from one product to another. Due to discrepant designs and techniques, there is not obvious relation among resolution, sampling rate and sampling error. ADCs whose resolution range from 8 bit to 16 bit and sampling rate range from 1 MHz to 40 MHz can satisfy most design requirements, so we chose those kinds of ADCs as our analysis targets in this paper. Detailed parameters of ADCs are shown in Table 2.

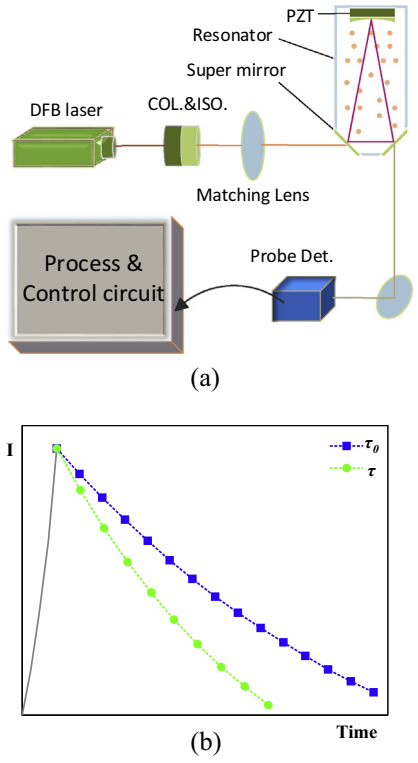

Fig. 1. (a) Conceptual schematic of CW-CRDS experimental setup, (b) illustration of photon intensity in resonator, where τ_0 and τ is photo time constant in the case respectively without and with the sample gas.

Table 1
Relationship between τ and gas concentration at different reflectivity of mirrors.

Concentration (ppbv)	R = 0.9999	R = 0.99995	R = 0.99999
0	5555.56	11111.11	55555.56
1	0.15	0.60	15.14
5	0.76	3.03	75.61
30	4.54	18.14	450.61
80	12.09	48.25	1185.6
200	30.12	119.84	2872

Where 0 ppbv corresponds to τ_0 and others are decrements of τ_0, with unit of nanosecond.

Table 2
Parameters of mainstream ADCs.*

Resolution (bit)	Sampling rate(MHz)	Sampling error (LSB)
8	1/4/10/40	0.2
12	1/4/10/40	0.7
16	1/4/10/40	1.2

* For simplicity, the input range is limited to 2 V peak–peak value for all. LSB: least significant bit.

3. Simulation

ADC converts analog signal to digital signal in a special frequency. From this simplified picture one might guess that different sampling interval can simulate sampling rate, and function truth values with random errors can substitute for sampling values. Decay curve of photon intensity in resonator is the simulation object. Detailed steps are as follows:

(1) According to the principle of CRDS, decay curve of photon intensity in resonator is given by:

$$y = a * \exp(-t/\tau), \tag{2}$$

where $a = 1$ and τ is photo time constants, as shown in Table 1.

(2) Generate sampling position sequence based on sampling rate of ADC.

(3) Calculate sampling value of y_n at each point in sequence generated in step (2) with formula (3) and formula (4):

$$y_n = y + err \tag{3}$$

$$\text{err} = \frac{V_{\text{pp}}}{2^{bit}} SE(2 * v1 - 1), \tag{4}$$

where y is function value at sampling point, err is random error, V_{pp} is the input voltage (peak-to-peak), bit is the resolution, SE is the sampling error, and $v1$ is a uniformly distributed random number between 0 and 1.

(4) Fit the simulation curve with objective function, given in step (1), in order to obtain photo time constant τ.

(5) Count distribution of τ on time axis.
(6) Repeat steps (3)–(5) until get enough fitting values.
(7) Compute the expectation and variance of τ.
(8) Repeat steps (1)–(7) for different resolutions and different sampling rates of ADCs. Combining with the photo time constant shown in Table 1, summarize guideline of ADC selection.

Fig. 2 provides an illustration of different distribution of τ. Parameters of ADC are shown in Table 2, with mirror reflectivity of 0.99999. Using gauss formula fitting, expectations and variances of τ are obtained and shown in Table 3:

The concentration of methane can be distinguished only when variance is lower than the corresponding value in Table 1. Combining Tables 1 and 3, for ADC with a 16 bit resolution and 4 MHz sampling rate, the variance is 10 ns with the reflectivity of 0.99999, which can distinguish concentration of methane of 1 ppbv (requiring variance less than 15.14 ns). If we merely want to distinguish concentration of methane of 30 ppbv, an ADC with 8 bit resolution and 4 MHz sampling rate is enough, despite a waste of high reflectivity of mirrors.

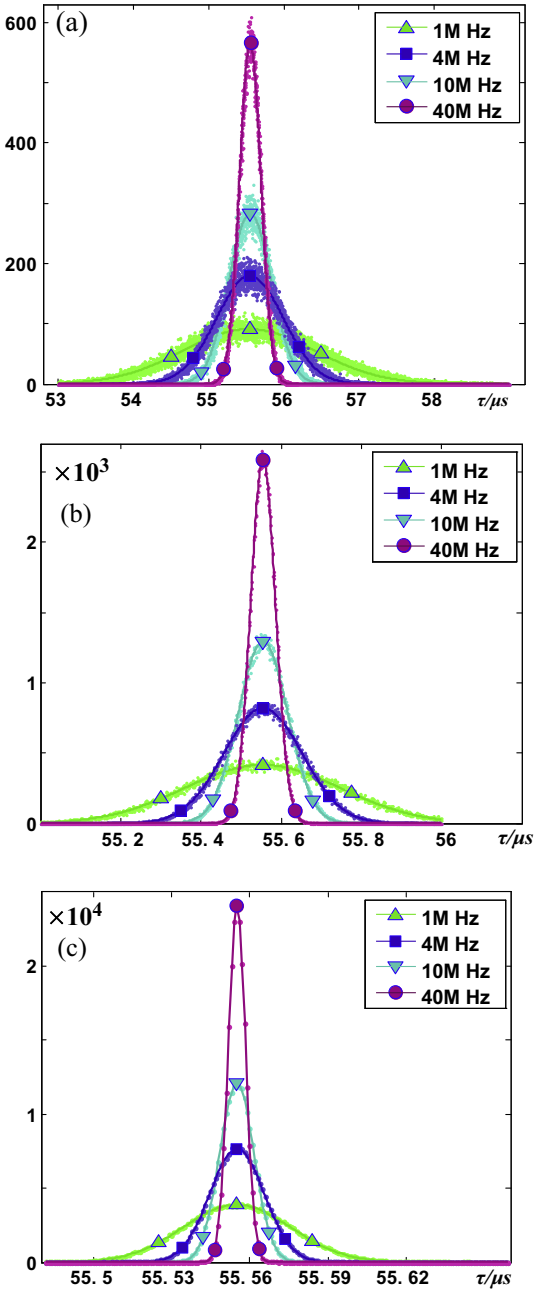

Fig. 2. Distributions of τ simulated with different resolutions and different sampling rates of ADCs. Resolutions in (a)–(c) are 8, 12 and 16 bit respectively.

Table 3
Expectations and variances of τ in Fig. 2.

Sampling rate (MHz)	8 bit	12 bit	16 bit
1	55.546 (0.877)	55.554 (0.195)	55.555 (0.021)
4	55.551 (0.445)	55.555 (0.097)	55.555 (0.010)
10	55.554 (0.282)	55.555 (0.062)	55.555 (0.007)
40	55.554 (0.141)	55.555 (0.031)	55.555 (0.003)

Where variances are shown in brackets. For simplicity, all variances keep the same significant digits, unless otherwise mentioned. Unit is microsecond.

As shown in Table 3, resolution of ADC has little effect on the expectation, so does the sampling rate. Variance decreases rapidly with the increase of resolution, while it decreases much slower with the increase of sampling rate. This can be figured out from the data itself. When the sampling accuracy is low, a relatively large amount of data is needed to average the random error. But the fitting accuracy will saturate as the number of data grow [21]. On the other hand, high fitting accuracy can also be obtained with a small amount of data of higher accuracy. Unfortunately, only improving the resolution of ADC is usually not enough to achieve expectant precision in practical application. The system noise with the same level of the sampling error of ADC is essential. It is easy to choose a high resolution ADC, but to improve the noise level of system is very difficult. We cannot get the nominal quantization precision of ADC due to the existence of system noise. The following experiments are designed to verify our hypothesis. Three ADCs with a resolution of 8 bit, 12 bit and 16 bit respectively are chosen for comparison, all with sampling rate of 10 MHz and sampling error of 0.5 LSB at 8 bit resolution. According to the simulation steps mentioned above, distributions of τ are shown in Fig. 3. It indicates that the same sampling error of ADC attains the same sampling precision.

It can be confirmed from Fig. 3 and Table 4 that sampling error is the core factor that determines the sampling precision. System

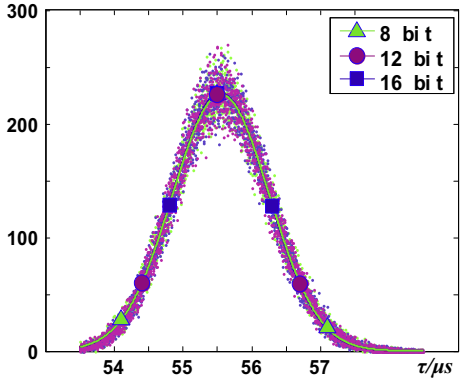

Fig. 3. Distributions of τ, simulated at different resolutions with same sampling error.

Table 4
Expectations and variances of τ in Fig. 3.

	8 bit	12 bit	16 bit
Expectation (μs)	55.552 (0.704)	55.548 (0.700)	55.548 (0.704)

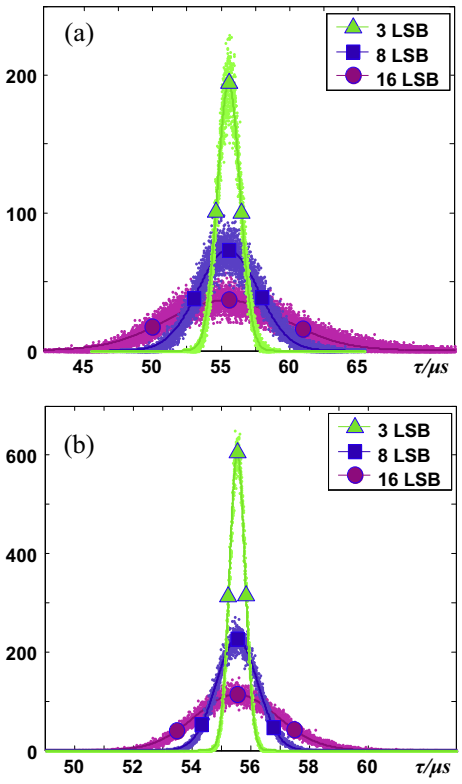

Fig. 4. Distributions of τ with different sampling errors. (a) Sampling rate of 1 MHz, (b) sampling rate of 10 MHz.

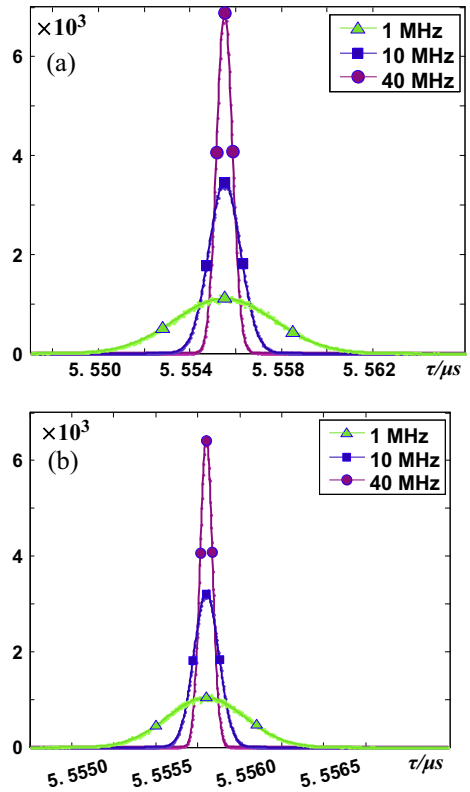

Fig. 5. Distributions of τ with reflectivity of 0.9999. (a) Resolution is 12 bit, (b) resolution is 16 bit.

Table 5
Expectations and variances of τ in Fig. 4.

Sampling rate (MHz)	3 LSB	8 LSB	16 LSB
1	55.548 (0.825)	55.508 (2.187)	55.382 (4.294)
10	55.554 (0.264)	55.550 (0.704)	55.535 (1.399)

Where unit is microsecond.

Table 6
Expectations and variances of τ in Fig. 5.

Sampling rate (MHz)	12 bit	16 bit
1	5555.50 (2.17)	5555.55 (0.23)
10	5555.51 (0.69)	5555.55 (0.07)
40	5555.51 (0.35)	5555.55 (0.03)

Where unit is nanosecond.

noise occupies the major portion of sampling error. The influence of sampling errors on distributions of τ are shown in Fig. 4 and Table 5. System noise is converted into ADC sampling error, and the resolution of ADC is 12 bit.

Fig. 4 and Table 5 show how sampling error and sampling rate influence on the distributions of photo time constant τ. The larger quantization error, the lower expectation accuracy is. By merely increasing the sampling rate, accuracy of τ can only be improved to a certain degree.

Besides the parameters of ADC, target fitting functions also have effects on fitting accuracy. For example, when reflectivity of mirror decreases to 0.9999, the photo time constant reduces to 5555.56 ns. A 0.15 ns fitting resolution is needed to distinguish concentration of methane of 1ppbv as shown in Table 1. Simulation result of 12 bit ADC with sampling error of 0.7 LSB is shown in Fig. 5(a), and simulation result of 16 bit ADC with sampling error of 1.2 LSB is shown in Fig. 5(b). Combining Tables 1 and 6, variance of ADC with a 16 bit resolution and 10 MHz sampling rate is 0.07 ns, which is enough to distinguish concentration of methane of 1 ppbv at this condition. Comparing Table 4 with Table 6, we can find that expectation decreases by 10 times, while variance reduces by 100 times.

4. Conclusions

ADC is the key component of AD-system, and its resolution and sampling rate directly determine the bit-width and the minimum operating frequency of digital system, which have great effect on circuit design. By fitting the photo time constant τ of CRDS system, we conclude that resolution of ADC has much more effect on fitting precision than sampling rate, reducing sampling error will get a best fitting precision, and in the selection of ADC individual objective fitting function should be considered. In addition, system noise should also be included into ADC sampling error to get nominal sampling accuracy. Therefore, according to above analysis, we can choose an ADC with suitable resolution and sampling rate enabling instrument working at optimal bit-width and frequency with designed sensitivity in indirect measurement.

Acknowledgments

We sincerely thank Zhaoqi Wang, Changxiang Yan, Peng Li and Lihong Cui for valuable advice and assistance. The work is supported by the National Key Scientific Instrument and Equipment Development Project, Nos. 2012YQ160185, and 2012ZX04001-011.

References

[1] J.M. Herbelin, J.A. McKay, M.A. Kwok, et al., Sensitive measurement of photon lifetime and true reflectances in an optical cavity by a phase-shift method, Appl. Opt. 19 (1) (1980) 144–147.

[2] A. O'Keefe, D.A. Deacon, Cavity ring-down optical spectrometer for absorption measurements using pulsed laser sources, Rev. Sci. Instrum. 59 (12) (1988) 2544–2551.

[3] R.J. Wild, P.M. Edwards, et al., A measurement of total reactive nitrogen, NO y, together with NO_2, NO, and O_3 via cavity ring-down spectroscopy, Environ. Sci. Technol. 48 (16) (2014) 9609–9615.

[4] E. Crosson, A cavity ring-down analyzer for measuring atmospheric levels of methane, carbon dioxide, and water vapor, Appl. Phys. B 92 (3) (2008) 403–408.

[5] G. Neri, A. Lacquaniti, et al., Real-time monitoring of breath ammonia during haemodialysis: use of ion mobility spectrometry (IMS) and cavity ring-down spectroscopy (Crds) techniques, Nephrol. Dial. Transplant. 27 (7) (2012) 2945–2952.

[6] K. Tanaka, R. Kojima, et al., Continuous measurements of stable carbon isotopes in CO_2 with a near-Ir laser absorption spectrometer, Infrared Phys. Technol. 60 (2013) 281–287.

[7] N.A. Yebo, S.P. Sree, et al., Selective and reversible ammonia gas detection with nanoporous film functionalized silicon photonic micro-ring resonator, Opt. Express 20 (11) (2012) 11855–11862.

[8] A. Grossel, V. Zéninari, et al., Photoacoustic detection of nitric oxide with a helmholtz resonant quantum cascade laser sensor, Infrared Phys. Technol. 51 (2) (2007) 95–101.

[9] V. Sanders, High-precision reflectivity measurement technique for low-loss laser mirrors, Appl. Opt. (1977).

[10] D.Z. Anderson, J.C. Frisch, C.S. Masser, Mirror reflectometer based on optical cavity decay time, Appl. Opt. 23 (8) (1984) 1238–1245.

[11] P. Zalicki, R.N. Zare, Cavity ring-down spectroscopy for quantitative absorption measurements, J. Chem. Phys. 102 (7) (1995) 2708–2717.

[12] D.A. Long, A. Cygan, et al., Frequency-stabilized cavity ring-down spectroscopy, Chem. Phys. Lett. 536 (2012) 1–8.

[13] http://www.picarro.com/products_solutions/trace_gas_analyzers/co_co2_ch4_h2o[OL] (accessed 17.04.15).

[14] Y. Li, O.V. Svitelskiy, et al., Giant resonant light forces in microspherical photonics, Light: Sci. Appl. 2 (4) (2013) e64.

[15] B.V. Benjamin, P. Gao, et al., Neurogrid: a mixed-analog-digital multichip system for large-scale neural simulations, Proc. IEEE 102 (5) (2014) 699–716.

[16] T.J. Cui, M.Q. Qi, et al., Coding metamaterials, digital metamaterials and programming metamaterials, Light: Sci. Appl. 3 (2014) e218.

[17] F. Bizzarri, A. Brambilla, G. Storti Gajani, Extension of the variational equation to analog/digital circuits: numerical and experimental validation, Int. J. Circuit Theory Appl. 41 (7) (2013) 743–752.

[18] J. Takala, W. Gross, W. Sung, Guest Editors' introduction to special issue on advances in DSP system design, J. Signal Process. Syst. 71 (3) (2013) 169–171.

[19] C. Jain, P. Morajkar, et al., Measurement of absolute absorption cross sections for nitrous acid (HONO) in the near-infrared region by the continuous wave cavity ring-down spectroscopy (cw-CRDS) technique coupled to laser photolysis, J. Phys. Chem. A 115 (39) (2011) 10720–10728.

[20] http://www.analog.com/en/products/analog-to-digital-converters/ad-converters.html[OL] (accessed 17.04.15).

[21] C. Xiru, Probability theory and mathematical statistics, Press of USTC, 1991.